Materials Physics and Mechanics. 2022;50(4): 401-409
Research article
http://dx.doi.org/10.18149/MPM.5032022_4

Submitted: July 18, 2022
Approved: September 19, 2022
Accepted: November 23, 2022

The void evolution kinetics driven by residual stress in icosahedral particles

A.S. Khramov[1], S.A. Krasnitckii[2*], A.M. Smirnov[1,3], M. Yu. Gutkin[1,3,4]

[1]ITMO University, St. Petersburg, 197101, Russia

[2]St. Petersburg State University, St. Petersburg, 199034, Russia

[3]Peter the Great St. Petersburg Polytechnic University, St. Petersburg, 195251, Russia

[4]Institute for Problems in Mechanical Engineering, Russian Academy of Sciences, St. Petersburg, Russia

*krasnitsky@inbox.ru

Abstract. A kinetic model of vacancy diffusion induced by both the Gibbs-Thompson curvature effect and stress state of the Marks-Ioffe stereo-disclination in a hollow spherical particle is suggested to investigate the void evolution in hollow icosahedral particles. The obtained analytically vacancy concentration profile inside the hollow icosahedral particle is employed to derive numerically the evolution equation of void kinetics. It is shown that the scenario of void evolution in icosahedral particles strongly depends on the inner-to-outer radius ratio at the initial moment of time and on the value of dimensionless parameter α reflecting the contribution of a pressure-induced (drift) vacancy flux between the external and internal particle surfaces.

Keywords: Icosahedral small particles, residual stress, stress relaxation, disclination, hollow particles, spherical pore, pressure-induced diffusion

Acknowledgements*. Acknowledgements. This work was supported by the Russian Science Foundation (grant No. 22-11-00087, https://rscf.ru/en/project/22-11-00087/).*

Citation: Khramov AS, Krasnitckii SA, Smirnov AM, Gutkin MY. The void evolution kinetics driven by residual stress in icosahedral particles. *Materials Physics and Mechanics*. 2022;50(3): 401-409. DOI: 10.18149/MPM.5032022_4.

Introduction

Hollow and porous nanostructures have aroused a keen interest due to their higher performance in the various fields as plasmonics [1], nanosensing [2], energy storing [3], catalysis [4] and medicine [5] than their solid counterparts. By now, a large number of reviews (see, for example, [6-9]) has been devoted to different aspects of synthesis of hollow nanostructures as well as the influence of hollows on the functional properties of the devices based on these nanostructures. However, the theoretical aspects of void evolution are still of great concern being limited by following issues [10]: void shrinkage due to the Gibbs-Thompson curvature effect in single-crystalline (SCPs) and polycrystalline (PCPs) particles of pure elements [11-16], void growth due to the nanoscale Kirkendall effect in bi-metallic [12,17-19] and oxidated [20-22] particles, void formation as a residual stress relaxation mechanism in multiply twinned particles (MTPs) [23-28]. The latter phenomenon was effectively investigated by quasi-equilibrium energetic approach in pentagonal whiskers (PWs), icosahedral (IcPs) [25] and decahedral particles (DhPs) [28] with respect to the disclination concept.

According to the disclination concept [29-31], the residual stress in an IcP can be described in terms of Marks-Ioffe stereo disclination (SD) with strength $\chi \approx 0.0613$ sr spread

Publisher: Peter the Great St. Petersburg Polytechnic University

over the volume of the elastic sphere [32]. Whitin this model, the interior region of IcP is subject to hydrostatical compression while the periphery region is subject to hydrostatical tension. This residual stress state induces the generation of vacancies on external particle surface and their subsequent migration to IcP central region. The vacancy saturation in particle central region can cause the void formation. From the energetical point of view, the void formation should decrease the stored strain energy and it seems to be an effective channel of residual stress relaxation in IcPs.

The void formation in IcPs was experimentally investigated by electron microscopy in [33-35]. Yasnikov and Vikarchuk in [33] employed chemical etching to examine porous structures in Cu IcPs produced by electrodeposition method. The voids were revealed in relatively big IcPs (with outer diameter more than ~1 μm) while relatively small IcPs (with outer diameter less than ~1 μm) were void-free. Besides, Huang *et al.* [35] investigated the influence of residual stress on the void formation and growth in bimetallic particles with icosahedral and octahedral shapes. It was shown that heating of a mixture of solid strained icosahedral Pd particles in Cu solution can be employed to synthesize hollow Pd-Cu alloyed particles, while heating of a mixture of strain-free solid octahedral Pd particles in the Cu solution did not lead to void formation and, on the contrary, the solid Pd/Cu core-shell particles were performed. This means that the void occurrence in particles strongly depends on the residual stress induced by multiply cycling twinning.

The aforementioned quasi-equilibrium energetic models [25,28] have not taken into account the influence of the vacancy diffusion on the void formation process in MTPs. An attempt to overcome this limitation was made in [24,26] for PWs and [27] for IcPs. Vlasov and Fedik [26] applied the bulk diffusion theory to investigate the initial-stage kinetics of void nucleation in PWs via the migration of vacancies under the stress state induced by a positive partial wedge disclination (WD). It was shown that the void growth rate at the initial stages in PWs obeys the parabolic low. Romanov and Samsonidze [24] considered the diffusion value problem in cylinder subjected to an elastic field of a WD with regard to presence of vacancy sinks/sources. The boundary conditions for vacancy concentration were prescribed by the WD stress field. Tsagrakis *et al.* [27] were the first who figured out the stress field of Mark-Ioffe SD in terms of strain-gradient elasticity. The obtained nonsingular analytical expression of the SD hydrostatic stress was employed to determine the vacancy concentration in IcPs in terms of diffusion associated theory. The main drawback of the discussed above kinetic models of void evolution in MTPs, however, is the fact that they have not taken into consideration the vacancy concentration gradient induced by the Gibbs-Thomson curvature effect on external and internal particle surfaces, although it is well known that this effect is responsible for void shrinking process observed experimentally [36,37] and within computer simulations [38-40].

This work aims at investigating the void evolution kinetics in IcPs in terms of counteraction of the Gibbs-Thomson curvature effect [11] and the relaxation of residual stress [32]. In order to do this, an analytical solution of the boundary value problem of bulk diffusion of vacancies in the spherical shell with respect to both the Gibbs-Thompson surfaces conditions and the stress state of Marks-Ioffe SD is obtained. This solution is employed to elucidate the scenarios of void evolution kinetics in hollow IcPs.

Model

We consider a bulk diffusion kinetics of the vacancies in a single element isotropic spherical shell with inner and outer radii a_p and a subjected to stress state of a Marks-Ioffe SD with strength $\chi \approx 0.0613$ (see Fig.1). The total vacancy flux density [$m^{-2}s^{-1}$] inside the shell can be presented as a sum:

$$\mathbf{j}_v = \mathbf{j}_c + \mathbf{j}_\sigma , \qquad (1)$$

where

$$\mathbf{j}_c = -\frac{D}{\Omega}\nabla C\,, \tag{2}$$

is the outward vacancy flux density corresponding to vacancy concentration gradient between the internal and external spherical shell surfaces, and

$$\mathbf{j}_\sigma = -\frac{D\,\delta v}{kT\,\Omega} C \nabla \sigma_\chi\,, \tag{3}$$

is the inward vacancy flux density corresponding to residual stress state of the IcP, D is the vacancy diffusion coefficient [m^2/s], $C = C(\boldsymbol{R}, t)$ is the dimensionless relative concentration of vacancies, $\boldsymbol{R}$ is the position-vector, t is the time, Ω is the atomic volume corresponding to the vacancy, δv is the vacancy relaxation volume, σ_χ is the hydrostatic stress induced by the Marks-Ioffe stereo disclination, kT has its usual meaning, and ∇ is the nabla operator. The void evolution scenario is defined by the contribution of each term in Eq.1: (i) shrinkage if $|\mathbf{j}_c| > |\mathbf{j}_\sigma|$, (ii) growth if $|\mathbf{j}_\sigma| > |\mathbf{j}_c|$, and (iii) equilibrium if $|\mathbf{j}_\sigma| = |\mathbf{j}_c|$.

The rate of vacancy concentration inside the shell is goverend by the mass conservation law

$$\frac{\partial C}{\partial t} + \nabla \cdot (\Omega\, \mathbf{j}_v) = 0\,. \tag{4}$$

Substituting Eqs.1-3 in Eq.4 and taken into consideration the steady state process assumption ($\partial C/\partial t \approx 0$) one can obtain the Fick second law in the following form:

$$\nabla^2 C + \frac{\delta v}{kT}\nabla \cdot (C \nabla \sigma_\chi) = 0 \tag{5}$$

According to the classical Gibbs-Thomson effect in hollow SCPs, vacancies tend to migrate from the internal surface to the external surface causing the void shrinkage with subsequent void collapse. The influence of this phenomenon on the void evolution kinetics in hollow particles can be introduced in terms of the boundary condition for Eq.5 at the internal and external shell surfaces in the linear form of the Gibbs-Thompson conditions [11]:

$$C(a_p) = C_0\left(1 + \frac{\beta}{a_p}\right),\quad C(a) = C_0\left(1 - \frac{\beta}{a}\right), \tag{6a,b}$$

where C_0 is the equilibrium vacancy concentration in vicinity of a planar surface, $\beta = 2\gamma\,\Omega/kT$, and γ is the specific surface energy.

The pressure-induced (drift) vacancy flux from the external IcP surface to the internal one is determined by the hydrostatic component of the SD stress tensor ($\sigma_\chi = -1/3\ \mathrm{tr}\,\boldsymbol{\sigma}$). In accordance with the continuum model of a hollow IcP [32], the hydrostatic stress can be written as

$$\sigma_\chi = \frac{4G\chi(1+\nu)}{3(1-\nu)}\left[\frac{1}{3} + \ln\frac{R}{a} + \frac{a_p^3}{a^3 - a_p^3}\ln\frac{a_p}{a}\right], \tag{7}$$

where G is the shear modulus, ν is the Poisson ratio, and $R = |\mathbf{R}|$. The gradient of the hydrostatic stress is given by

$$\nabla \sigma_\chi = \frac{4G\chi(1+\nu)}{3(1-\nu)}\frac{\mathbf{R}}{R^2}\,. \tag{8}$$

Then the equation of the Fick second law in spherical coordinate systems for a hollow particle subjected to the SD stress fields in the steady-state process assumption reads

$$\frac{d^2C}{dR^2} + \frac{2-\alpha}{R}\frac{dC}{dR} - \frac{\alpha C}{R^2} = 0\,, \tag{9}$$

where

$$\alpha = \frac{G\chi}{3}\frac{1+\nu}{1-\nu}\frac{\delta v}{kT}\,. \tag{10}$$

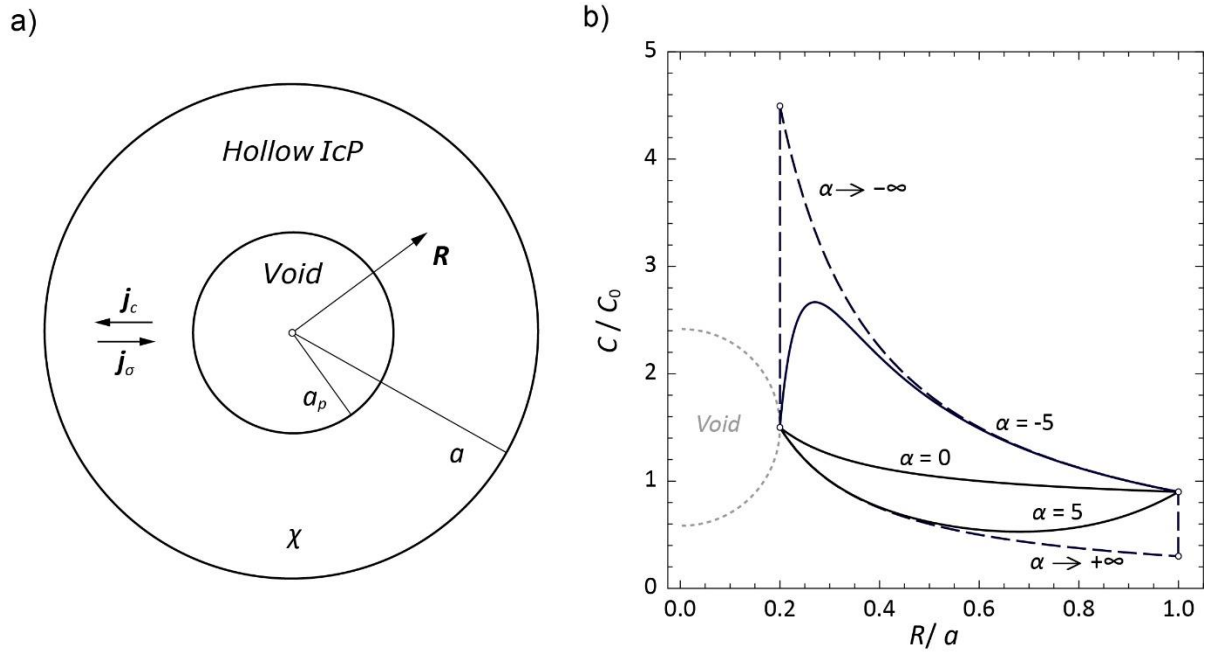

Fig. 1. a) The continuum model of an IcP containing a central spherical void. b) The dependences of normalized vacancy concentration on dimensionless radial coordinate R/a in the IcP with $a_p/a = 0.2$ and $\beta/a = 0.1$ given for different values of parameter $\alpha = 0, \pm 5$ and for $\alpha \to \pm\infty$

Thus, the vacancy diffusion in hollow IcPs can be described by Eq.9 under the boundary condition given by Eq.6.

Results

One can obtain the analytical solution of Eq.9 under the boundary conditions (Eqs.6a,b) on the internal and external surfaces in the following form

$$C = C_0 \frac{(a_p + \beta)(a^{1+\alpha} - R^{1+\alpha}) + (a - \beta)(R^{1+\alpha} - a_p^{1+\alpha})}{(a^{1+\alpha} - a_p^{1+\alpha})R}. \quad (11)$$

In the case of $\alpha \to 0$, Eq.11 transforms to the expression obtained in work [11] for stress-free hollow SCPs.

Fig. 1b demonstrates the vacancy concentration profiles in a hollow IcP with the ratio of inner to outer radii $a_p/a = 0.2$, calculated from Eq.11 for $\beta/a = 0.1$ and different values of α. As is seen from Fig.1b, the presence of the SD stress state ($\alpha < 0$) induces a local increase of vacancy concentration in vicinity of the internal particle surface. In the limiting case of $\alpha \to -\infty$, the contribution of concentration flux is negligible small (the vacancy flux is completely determined by the drift term), and the vacancy concentration reaches the highest value ~4.5C_0 at the internal surface ($R = a_p$). It is worth noting that diffusion of impurities (here we mean interstitial atoms or substitutional impurity atoms of radius greater than the radius of the parent atoms) in IcPs can be described by positive values of α. Fig.1b shows that the values of impurity concentration in hollow IcPs always less than those in SCPs. Besides, the minimum value of impurity concentration tends to move to the external surface with an increase in α. In the limiting case of $\alpha \to +\infty$, the impurity concentration takes a constant value ~0.3C_0 at the outer surface of the hollow IcP.

Turn now to the void evolution kinetics in IcPs. The rate of the inner surface can be determined by vacancy flux at the void surface from Eqs.1-3 in the following form

$$\frac{da_p}{dt} = -\Omega \frac{\mathbf{j}_v \cdot \mathbf{R}}{R}\bigg|_{R=a_p} = \frac{(1+\alpha)C_0 D}{a_p^2} \frac{(a_p+\beta)a^{1+\alpha} - (a-\beta)a_p^{1+\alpha}}{a^{1+\alpha} - a_p^{1+\alpha}}. \quad (12)$$

Let us rewrite Eq.12 as

$$\frac{dp}{d\tau} = -\frac{(1+\alpha)\Delta^5}{bp^2} \frac{(p+b\Delta) - (1-b\Delta)p^{1+\alpha}}{1-p^{1+\alpha}}, \quad (13)$$

where the following dimensionless variables are introduced

$$p = \frac{a_p}{a}, \qquad \tau = \frac{C_0 D\beta t}{a_0^3}, \qquad \Delta = (1-p^3)^{1/3}, \qquad b = \frac{\beta}{a_0}, \quad (14a\text{-}d)$$

where a_0 is the radius of a void-free particle

$$a_0 = (a^3 - a_p^3)^{1/3}. \quad (15)$$

Eq.15 claims that the particle remains unchanged during the void evolution processes.

The solution of Eq.13 was obtained by numerical integration and illustrated in Fig.2a. The curves $p(\tau)$ are shown for different values of α and initial normalized void radius $p_0 = a_{p,0}/a$. As is seen from Fig.2a, the scenario of void evolution in IcPs is strongly determined by the initial void radius and the value of α. In the case of $\alpha = 0$, for any values of p_0, the void tends to shrinkage and finally collapses at the time $\tau = \tau_f$ as it was shown in [12,13]. For $\alpha = -0.5$, the void tends to reach some equilibrium size $p_{eq} = a_{p,eq}/a$ via growing (when $p_0 < p_{eq}$) or shrinking (when $p_0 > p_{eq}$). It is worth noting that, for relatively small values of $\alpha < -1$, solid IcPs could be transformed into thin spherical shells (see, for example, the curve for $\alpha = -2$) as it was observed experimentally in [33].

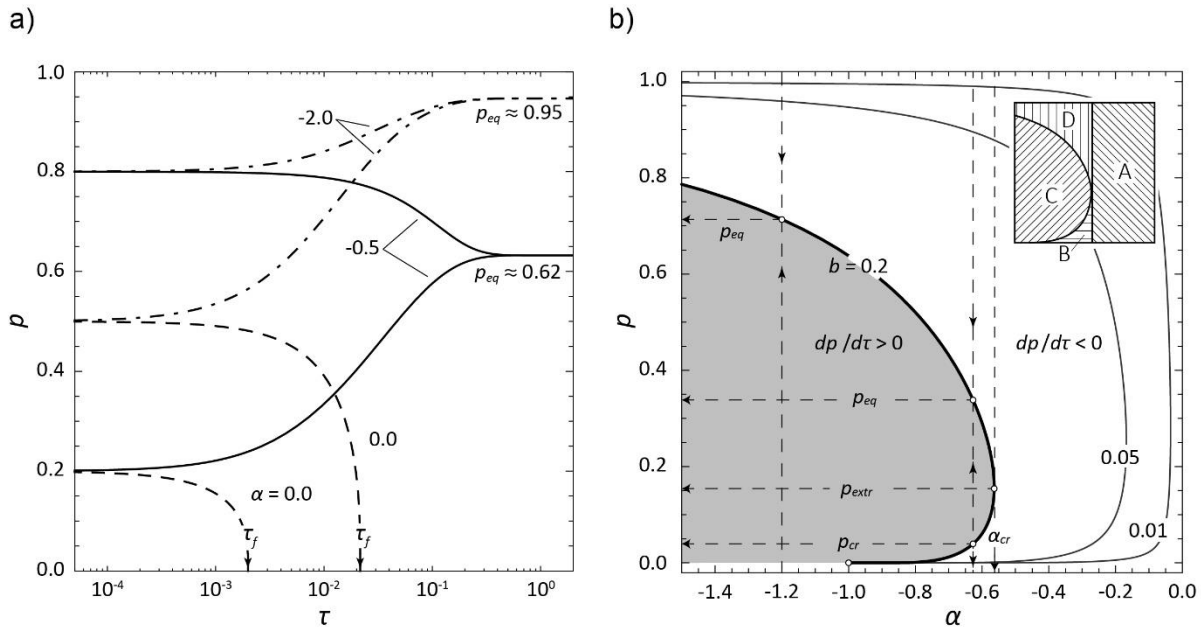

Fig. 2. a) Dependence of the normalized void radius $p = a_p/a$ on the dimensionless time τ at $b = 0.1$ for different values of the initial IcP radii ratio $p_0 = 0.2$, 0.5, and 0.8, and $\alpha = 0.0$ (dashed curves), –0.5 (solid curves), –2.0 (dashed-and-dotted curves). b) The curves $dp/d\tau = 0$ in dependence on the normalized void radius p and the parameter α for different values of $b = 0.01$, 0.05, 0.2. The inset in the upper right corner demonstrates the regions A, B, C and D corresponding to different pathways of the void evolution

The void growth or shrinkage scenarios are determined by the sign of $dp/d\tau$ in Eq.13. In order to analyze possible pathways of void evolution in IcPs, the condition $dp/d\tau = 0$ was considered. Then from Eq.13 one gets

$$1+\alpha = \log_p \frac{p+b\Delta}{1-b\Delta}. \quad (16)$$

In Fig.2b, the curves $f(\alpha, p)$ satisfying Eq.16 for different values of b are shown. As is seen from Fig.2b, the void tends to grow if p_0 and α values are in the area $dp/d\tau > 0$; in contrast, the void tends to shrink if p_0 and α values are in the area $dp/d\tau < 0$. Therefore, one can define the regions in Fig.2b according to the following void evolution scenarios: A) the void tends to shrink with collapse for any values of the initial void ratio if α exceeds some critical value α_{cr} ($\alpha > \alpha_{cr}$, $0 < p_0 < 1$). Besides, the critical parameter $\alpha_{cr} \to 0$ if b decreases; B) there is a critical value of the normalized void radius, p_{cr}, bellow which the void nucleus shrinks to collapse ($-1 < \alpha < \alpha_{cr}$, $0 < p_0 < p_{cr}$); C) for ($-1 < \alpha < \alpha_{cr}$, $p_{cr} \le p_0 < p_{eq}$) or ($\alpha < -1$, $0 < p_0 < p_{eq}$), the void grows to get the optimal (equilibrium) normalized radius p_{eq}; D) for ($\alpha < \alpha_{cr}$, $p_0 > p_{eq}$), the void shrinks to get the optimal normalized radius p_{eq}.

Thus, the void is unstable in regions A and B – here a hollow IcP has a tendency to transform in a compact particle with radius a_0. On the contrary, the void has an optimal size in regions C and D – the void in an IcP has a tendency to change its volume until reaching the equilibrium radius $a_{p,eq}$.

Conclusions

In summary, we have considered the vacancy diffusion in hollow IcPs to analyze the void evolution kinetics. The vacancy flux is defined by concentration gradient and pressure-induced (drift) terms. The first term is caused by the difference between vacancy concentrations at the inner and outer particle surfaces due to the Gibbs-Thompson curvature effect. The second term is determined by the residual stress state and described by the Marks-Ioffe SD elastic model of a hollow IcP. The contribution of each term in vacancy diffusion is defined by a dimensionless parameter α: the drift diffusion prevails over the concentration one if $\alpha << -1$, vice versa if $\alpha \to 0$, and the contributions of both the terms are comparable if $\alpha \approx 0$. An analytical solution of the corresponding boundary value problem of bulk diffusion is given for the radial dependence of vacancy concentration. It is demonstrated that in IcPs, a local vacancy saturation is observed in vicinity of the void surface. The analytical expression for vacancy profile is employed to obtain the equation of void evolution. It is shown that the scenario of void evolution in IcPs strongly depends on the initial void radius $a_{p,0}$ as well as the value of parameter α. There is such a critical parameter α_{cr} that, for $\alpha > \alpha_{cr}$, the void has a tendency to shrink with subsequent collapse for any initial void radius $a_{p,0}$. When $\alpha < \alpha_{cr}$, the following processes can occur: (i) the void shrinkage with subsequent collapse, if the initial void radius is less than its critical value, $a_{p,0} < a_{p,cr}$; (ii) the void shrinkage until reaching its optimal size, if the initial void radius is larger than its equilibrium value, $a_{p,0} > a_{p,eq}$; and (iii) the void growth until reaching its optimal size, if the initial void radius is in the interval $a_{p,cr} < a_{p,0} < a_{p,eq}$.

References

1. Genç A, Patarroyo J, Sancho-Parramon J, Bastús NG, Puntes V, Arbiol J. Hollow metal nanostructures for enhanced plasmonics: synthesis, local plasmonic properties and applications. *Nanophotonics*. 2017;6(1): 193-213.

2. Wang T, Kou X, Zhao L, Sun P, Liu C, Wang Y, Shimanoe K, Yamazoe N, Lu G. Flower-like ZnO hollow microspheres loaded with CdO nanoparticles as high performance sensing material for gas sensors. *Sensors and Actuators B: Chemical*. 2017;250: 692-702.

3. Zhu C, Wang H, Guan C. Recent progress on hollow array architectures and their applications in electrochemical energy storage. *Nanoscale Horizons*. 2020;5(8): 1188-1199.
4. Fu J, Detsi E, De Hosson JTM. Recent advances in nanoporous materials for renewable energy resources conversion into fuels. *Surface and Coatings Technology*. 2018;347: 320-336.
5. Yasun E, Gandhi S, Choudhury S, Mohammadinejad R, Benyettou F, Gozubenli N, Arami H. Hollow Micro and Nanostructures for Therapeutic and Imaging Applications. *Journal of Drug Delivery Science and Technology*. 2020;60: 102094.
6. Anderson BD, Tracy JB. Nanoparticle conversion chemistry: Kirkendall effect, galvanic exchange, and anion exchange. *Nanoscale*. 2014;6(21): 12195-12216.
7. Wang X, Feng JI, Bai Y, Zhang Q, Yin Y. Synthesis, properties, and applications of hollow micro-/nanostructures. *Chemical Reviews*. 2016;116(18): 10983-11060.
8. Yu L, Yu XY, Lou XW. The Design and Synthesis of Hollow Micro-/Nanostructures: Present and Future Trends. *Advanced Materials*. 2018;30(38): 1800939.
9. Zhu M, Tang J, Wei W, Li S. Recent progress in the syntheses and applications of multishelled hollow nanostructures. *Materials Chemistry Frontiers*. 2020;4(4): 1105-1149.
10. Krasnitckii SA, Gutkin MY. Review on theoretical models of void evolution in crystalline particles. *Reviews on Advanced Materials and Technologies*. 2021;3(1): 96-126.
11. Tu KT, Gösele U. Hollow nanostructures based on the Kirkendall effect: design and stability considerations. *Applied Physics Letters*. 2005;86(9): 093111.
12. Gusak AM, Zaporozhets TV, Tu KT, Gösele U. Kinetic analysis of the instability of hollow nanoparticles. *Philosophical Magazine*. 2005;85(36): 4445-4464.
13. Evteev AV, Levchenko EV, Belova IV, Murch GE. Shrinking kinetics by vacancy diffusion of a pure element hollow nanosphere. *Philosophical Magazine*. 2007;87(25): 3787-3796.
14. Fischer FD, Svoboda J. High temperature instability of hollow nanoparticles. *Journal of Nanoparticle Research*. 2008;10(2): 255-261.
15. Yanovsky VV, Kopp MI, Ratner MA. Gas-filled pore in bounded particle. *Arxiv*. [Preprint] 2019. Available from: https://doi.org/10.48550/arXiv.1910.13956.
16. Klinger L, Murch GE, Belova IV, Rabkin E. Pores shrinkage and growth in polycrystalline hollow nanoparticles and nanotubes. *Scripta Materialia*. 2020;180: 93-96.
17. Evteev AV, Levchenko EV, Belova IV, Murch GE. Formation of a hollow binary alloy nanosphere: a kinetic Monte Carlo study. *Journal of Nano Research*. 2009;7: 11-17.
18. Yu HC, Yeon DH, Li X, Thornton K. Continuum simulations of the formation of Kirkendall-effect-induced hollow cylinders in a binary substitutional alloy. *Acta Materialia*. 2009;57(18): 5348-5360.
19. Jana S, Chang JW, Rioux RM. Synthesis and modeling of hollow intermetallic Ni–Zn nanoparticles formed by the Kirkendall effect. *Nano Letters*. 2013;13(8): 3618-3625.
20. Fischer FD, Svoboda J. Modelling of reaction of metallic nanospheres with gas. *Solid State Phenomena*. 2011;172: 1028-1037.
21. Levitas VI, Attariani H. Mechanochemical continuum modeling of nanovoid nucleation and growth in reacting nanoparticles. *The Journal of Physical Chemistry C*. 2012;116(1): 54-62.
22. Klinger L, Kraft O, Rabkin E. A model of Kirkendall hollowing of core-shell nanowires and nanoparticles controlled by short-circuit diffusion. *Acta Materialia*. 2015;83: 180-186.
23. Mikhailin AI, Romanov AE. Amorphization of disclination core. *Sov. Physics of the Solid State*. 1986; 28(2): 601–603.
24. Romanov AE, Samsonidze GG. Diffusion in the elastic field of a wedge disclination. *Sov. Technical Physics Letters*. 1988;14(14): 585-586.
25. Romanov AE, Polonsky IA, Gryaznov VG, Nepijko SA, Junghanns T, Vitrykhovski NJ. Voids and channels in pentagonal crystals. *Journal of Crystal Growth*. 1993;129: 691-698.
26. Vlasov NM, Fedik II. Diffusion-induced relaxation of residual stresses. *Doklady Physics*. 2000;45(11): 623-626.

27. Tsagrakis I, Yasnikov IS, Aifantis EC. Gradient elasticity for disclinated micro crystals. *Mechanics Research Communications.* 2018;93: 159-162.
28. Krasnitckii SA, Gutkin MY, Kolesnikova AL, Romanov AE. Formation of a pore as stress relaxation mechanism in decahedral small particles. *Letters on Materials*. 2022;12(2): 137-141.
29. Wit RDe. Partial disclinations. *Journal of Physics. C. Solid State Physics*. 1972;5: 529-534.
30. Romanov AE, Kolesnikova AL. Application of disclination concept to solid structures. *Progress in Material Science*. 2009;54: 740–769.
31. Romanov AE, Kolesnikova AL. Elasticity Boundary-Value Problems for Straight Wedge Disclinations. A Review on Methods and Results. *Reviews on Advanced Materials and Technologies.* 2021;3(1): 55-95.
32. Howie A, Marks LD. Elastic strains and the energy balance for multiply twinned particles. *Philosophical Magazine A*. 1984;49(1): 95-109.
33. Yasnikov IS, Vikarchuk AA. Voids in icosahedral small particles of an electrolytic metal. *Journal of Experimental and Theoretical Physics Letters*. 2006;83(1): 42-45.
34. Wang X, Figueroa-Cosme L, Yang X, Luo M, Liu J, Xie Z, Xia Y. Pt-based icosahedral nanocages: using a combination of {111} facets, twin defects, and ultrathin walls to greatly enhance their activity toward oxygen reduction. *Nano Letters*. 2016;16(2): 1467-1471.
35. Huang J,.Yan Y, Li X, Qiao X, Wu X, Li J, Zhang H. Unexpected Kirkendall effect in twinned icosahedral nanocrystals driven by strain gradient. *Nano Research*. 2020;13(10): 2641-2649.
36. Nakamura R, Tokozakura D, Lee JG, Mori H, Nakajima H. Shrinking of hollow Cu_2O and NiO nanoparticles at high temperatures. *Acta Materialia*. 2008;56(18): 5276-5284.
37. Glodán G, Cserháti C, Beke DL. Temperature-dependent formation and shrinkage of hollow shells in hemispherical Ag/Pd nanoparticles. *Philosophical Magazine*. 2012;92(31): 3806-3812.
38. Wang Y, Liu Q, Sun Y, Wang R. Magnetic field modulated SERS enhancement of CoPt hollow nanoparticles with sizes below 10 nm. *Nanoscale*. 2018;10(26): 12650-12656.
39. Valencia FJ, Ramírez M, Varas A, Rogan J. Understanding the stability of hollow nanoparticles with polycrystalline shells. *The Journal of Physical Chemistry C*. 2020;124(18): 10143-10149.
40. Jiang C, Mo Y, Wang H, Li R, Huang M, Jiang S. Molecular dynamics simulation of the production of hollow silver nanoparticles under ultrafast laser irradiation. *Computational Materials Science.* 2021;196: 110545.

THE AUTHORS

Khramov A.S.
e-mail: 242531@niuitmo.ru
ORCID: 0000-0002-3895-0728

Krasnitckii S.A.
e-mail: Krasnitsky@inbox.ru
ORCID: 0000-0003-4363-8242

Smirnov A.M.
e-mail: andrei.smirnov@niuitmo.ru
ORCID: 0000-0002-7962-6481

Gutkin M. Yu.
e-mail: m.y.gutkin@gmail.com
ORCID: 0000-0003-0727-6352